CHARACTERIZATION OF THE MYOSIN ADENOSINE TRIPHOSPHATE (M·ATP) CROSSBRIDGE IN RABBIT AND FROG SKELETAL MUSCLE FIBERS

MARK SCHOENBERG
Laboratory of Physical Biology, National Institute of Arthritis and Musculoskeletal and Skin Diseases, Bethesda, Maryland 20892

ABSTRACT In the presence of ATP and absence of Ca^{2+}, muscle crossbridges have either MgATP or MgADP · P_i bound at the active site (S. B. Marston and R. T. Tregear, *Nature [Lond.]*, 235:22:1972). The behavior of these myosin adenosine triphosphate (M · ATP) crossbridges, both in relaxed skinned rabbit psoas and frog semitendinosus fibers, was analyzed. At very low ionic strength, $T = 5°C$, $\mu = 20$ mM, these crossbridges spend a large fraction of the time attached to actin. In rabbit, the attachment rate constants at low salt are $10^4 - 10^5$ s^{-1}, and the detachment rate constants are $\sim 10^4$ s^{-1}. When ionic strength is increased up to physiological values by addition of 140 mM potassium propionate, the major effect is a weakening of the crossbridge binding constant ~30–40-fold. This effect occurs because of a large decrease, ~100-fold, in the crossbridge attachment rate constants. The detachment rate constants decrease only 2–3-fold. The effect of ionic strength on crossbridge binding in the fiber is very similar to the effect of ionic strength on the binding of myosin subfragment-1 to unregulated actin in solution. Thus, the effect of increasing ionic strength in fibers appears to be a direct effect on crossbridge binding rather than an effect on troponin–tropomyosin. The finding that crossbridges with ATP bound at the active site can and do attach to actin over a wide range of ionic strengths strongly suggests that troponin–tropomyosin keeps a muscle relaxed by blocking a step subsequent to crossbridge attachment. Thus, rather than troponin–tropomyosin serving to keep a muscle relaxed by inhibiting attachment, it seems quite possible that the main way in which troponin–tropomyosin regulates muscle activity is by preventing the weakly-binding relaxed crossbridges from going on through the crossbridge cycle into more strongly-binding states.

INTRODUCTION

During the steady state hydrolysis of ATP by actomyosin, many distinct actin-myosin-nucleotide complexes are formed (Lymn and Taylor, 1971; Bagshaw and Trentham, 1974). These include the moieties formed immediately upon ATP binding, myosin adenosine triphosphate (M · ATP) and AM · ATP, the myosin-products complexes formed immediately upon hydrolysis, M · ADP · P_i and AM · ADP · P_i and the moieties formed as products are released, M · ADP, AM · ADP, M, and AM. It has been shown that in solution the M · ATP species, as well as the M · ADP · P_i species formed immediately upon hydrolysis, bind weakly to actin (Stein et al., 1979). The M · ADP and M states have been shown to bind strongly to actin (Highsmith, 1976; Marston et al., 1979; Greene and Eisenberg, 1980).

Over the years, considerable evidence has accumulated that states similar to those seen in solution exist in muscle fibers (Eisenberg and Greene, 1980; Hibberd and Trentham, 1986; Schoenberg, 1988). Previously it was shown that a crossbridge state having many of the properties of the M · ATP $\rightleftharpoons$ AM · ATP and MADP · P_i $\rightleftharpoons$ AMADP · P_i states seen in solution could be isolated and studied by examining relaxed fibers at very low ionic strength (Brenner et al., 1982; Schoenberg et al., 1984; Brenner et al., 1986; Schoenberg, 1988). That crossbridge state has alternatively been referred to as the weakly-binding state, the rapid-equilibrium state, or simply, the M · ATP state. It seems quite likely that the crossbridge state in the fiber that corresponds to the M · ATP state in solution is the species that forms the initial attachment with actin and it may even be the state that precedes the crossbridge power stroke. Thus, a detailed understanding of its kinetic properties would greatly enhance our understanding of the contractile cycle.

Recently (Schoenberg, 1985), several different ways for extracting the fiber crossbridge rate constants from mechanical measurements were discussed in detail. The present work applies one of these techniques to relaxed skinned rabbit psoas and also frog semitendinosus fibers in order to measure both the relative number of attached crossbridges and the crossbridge detachment rate constants at different ionic strengths. From this, the crossbridge attachment rate constants are also estimated. In agreement with previous studies (Brenner et al., 1982; Schoenberg et al., 1984), it was found that the crossbridge attachment and detachment rate constants are such that, at low ionic strength, the crossbridges in a relaxed fiber spend a large fraction of the time attached to actin. It was found further that increasing ionic strength to physiological values causes a large decrease in the crossbridge attachment rate constants. This results in the crossbridges

spending significantly less time attached to actin at physiological ionic strength. The number of crossbridges attached under different conditions correlates well with the biochemically-measured binding constant of myosin subfragment-1 to actin in solution. It does not correlate with the resting tension of the fiber. This suggests that both at low and normal ionic strength, the rapid stiffness of relaxed fibers at normal sarcomere length is due to weakly-binding rapid-equilibrium crossbridges. It suggests further that these relaxed crossbridges are in states which correspond to the weakly-binding S1 · ATP and S1 · ADP · P_i states seen in solution, and that they attach to and detach from the actin filament over a wide range of ionic strengths. Since the crossbridges continually attach to actin in a relaxed fiber even at normal ionic strength, a key step in muscle regulation must be subsequent to crossbridge attachment.

This work was presented, in part, at a symposium on the Molecular Mechanism of Muscle Contraction, held in Hakone, Japan, October 27–31, 1986 (Schoenberg, 1988).

THEORY

Since, in this paper, the magnitude of the attachment and detachment rate constants of the relaxed M · ATP crossbridge and how they vary with ionic strength is explored, it will be useful to briefly summarize the theoretical results upon which the analysis is based. One of the important results that came from previous modeling of rapid-equilibrium crossbridges (Schoenberg, 1985) is that the response of the crossbridges to mechanical strain is dominated by the crossbridge detachment rate constants. The attachment rate constants mainly affect the number of crossbridges attached. Intuitively, this occurs because the mechanical response to strain is due to crossbridges detaching and reattaching in positions of lesser strain. It is the most highly strained crossbridges that most often detach and reattach, and it is the detachment of these highly strained (high force-producing) bridges that tends to dominate the force response. The reattaching crossbridges tend not only to attach to the actin filament in positions of lesser strain but also to attach in an equilibrium distribution that produces little net force.

Previously I defined the chord stiffness of a muscle fiber as the amount of force generated by a given stretch divided by the size of the stretch. If the duration of the stretch is such that half of the crossbridges detach before the stretch is complete, the force induced at the end of the stretch will be about half that that would have been induced if no crossbridges detached (Schoenberg, 1985). What this means is that if one plots chord stiffness, S_c, versus the logarithm of the duration of stretch, t_d, the position of the curve on the logarithmic axis will depend upon the crossbridge detachment rate constants, and the amplitude of the curve will depend upon the number of crossbridges attached. It is this important result that enables us to determine whether a particular intervention affects the attachment rate constants, the detachment rate constants, or both.

Previously (Schoenberg, 1985), using a relatively simple one-attached-state model, it was shown that if crossbridges are detaching with only a single rate constant, the relationship between chord stiffness and duration of stretch is

$$S_c^d = (n_b K / k_b t_d)\,[1 - \exp(-k_b t_d)], \qquad (1)$$

where S_c^d is the chord stiffness measured over a stretch distance d, n_b is the total number of attached crossbridges, K is the stiffness of a single bridge, k_b is the crossbridge detachment rate constant, and t_d is the duration of the stretch. It is straightforward to show that if the crossbridges are detaching with i different rate constants, one has, if n_j crossbridges detach with rate constant k_j,

$$S_c^d = (K/t_d) \sum_{j=1}^{i} (n_j/k_j)\,[1 - \exp(-k_j t_d)] \qquad (2)$$

Eqs 1 and 2 will be useful in estimating the crossbridge detachment rate constants from an S_c – log t_d plot. Eq 2 serves to approximate the case where different populations of crossbridges detach with different rate constants or the detachment rate constants vary with crossbridge strain. Note that both equations are independent of the attachment rate constant except in so far as the attachment rate constant influences the total number of attached crossbridges.

METHODS

Solutions and Fiber Preparation

Skinned rabbit psoas fibers were isolated and prepared as reported previously (Schoenberg and Eisenberg, 1985). The rabbit fibers were skinned (made permeable to the bathing solution) by keeping them in a skinning solution for over 30 min. The rabbit skinning solution, fashioned after that of Eastwood et al. (1979), contained 150 mM KPropionate , 3 mM MgAcetate, 3 mM Na_2ATP, 5 mM ethylenebis (oxyethylenenitrilo) tetraacetic acid (EGTA), 0.5 mM dithiothreitol (DTT), and 5 mM KH_2PO_4, pH 6.8 at 5°C. The frog fibers were skinned using a modification of the method of Julian et al., 1971. Ventral heads of the semitendinosus muscle from American grass frogs (rana pipiens) were isolated and tied, via the tendons, to a Sylgard (Dow Corning Corp., Midland, MI) foundation. Enough chilled frog Ringer's solution (Schoenberg and Wells, 1984) to barely cover the whole muscle was applied, and to this, chilled frog skinning solution was added. The frog skinning solution was three parts rabbit skinning solution as described above and one part glycerol added to facilitate skinning. The skinning solution was added in aliquots initially as small as 100 μl in order to prevent the potassium in the solution from causing a contracture (Hodgkin and Horowicz, 1960). After a more than 100-fold excess of skinning solution was added, effectively diluting out the Ringer's solution, the muscle was incubated for 1 h. Subsequently, a single fiber was isolated, the glycerol-containing skinning solution was exchanged for glycerol-free relaxing solution, and the fiber was transferred to the experimental chamber for mounting as reported previously (Schoenberg and Eisenberg, 1985).

Low ionic strength relaxing solution contained 1 mM EGTA, 3 mM $MgCl_2$, 1 mM Na_2H_2ATP, 0.5 mM DTT, and 10 mM imidazole, pH 7.0. An additional 4 mM KCl was present because of separate pH adjustment of the individual constituents, making the total ionic strength of the

solution just under 20 mM. Higher ionic strength relaxing solutions were made by adding KPropionate. All rabbit fiber experiments were done at 5°C at a sarcomere length of 2.5 μm. The frog fiber experiments were done at 4°C and a sarcomere length of 2.4 μm.

Force Transducer. The force transducer was made from an AE801 force gage (Sensonor, Horten, Norway). The beam of the transducer was shortened 2.5–3 mm by gently grinding it against a piece of #600 emery paper rotating on a lathe. A 200 μm × 200 μm × 700 μm carbon–epoxy fiber was epoxied at the tip perpendicular to the silicon beam. It was to this that the muscle fiber was attached using a small amount of cyanoacrylic glue applied through a glass micropipette. After the experiment, the fiber and glue could be removed by applying acetone. The body of the transducer was held in a brass housing. Both the brass housing, the brass parts of the AE801, and the active elements of the transducer were pretreated with SS4004 primer and coated with RTV 60 silicone rubber compound (General Electric Co., Waterford, NY). This made them impervious to saline solution and insensitive to light.

The frequency response of the transducer was tested by releasing the tension on a small length of silk thread glued between the force transducer and displacement generator. For the different transducers used, the frequency response in water was generally 20–35 kHz and the damping time-constant was between 300–600 μs. The sensitivity was typically 10 mV/dyn, the high frequency noise was ~0.5 dyn, and the drift over 1 h was ~2 dyn. The total compliance of the system, including the displacement generator described below, was $<2 \times 10^{-3}$ μm/dyn.

Displacement Generator. The displacement generator was made from a 1.5 inch diameter speaker coil kindly provided by Acoustics Research (Cambridge, MA). The cloth dome covering the speaker coil was reinforced with epoxy and an 8-cm long, 2.5 mm diameter stainless steel extension epoxied in place. The movement of the dome and stainless steel extension was guided by two Y-shaped plastic leafsprings located 10 and 60 mm from the dome. Each arm of the leafspring measured 0.75 × 6 × 45 mm. When positioned in place, the stainless steel extension sat above the experimental chamber. Three 10 mm carbon-epoxy struts in an inverted tripod configuration formed a rigid vertical extension to the bath. At the tip of this, a very small horizontal carbon-epoxy fiber, similar to the one at the tip of the force transducer, was epoxied in place for mounting the muscle fiber. The displacement of the speaker was detected as described previously (Schoenberg et al., 1974). The half-time of the detector response was <3 μs.

Driving the Displacement Generator. The signal from the displacement transducer, in addition to being displayed, was fed forward to a LF356N operational amplifier (National Semiconductor, Santa Clara, CA) which calculated the difference between the speaker displacement and a command signal. This difference signal was then summed with a signal proportional to the first derivative of the displacement signal in order to generate the negative feedback signal to control the driving current to the speaker. The driving current, up to 7 A, was supplied by an HC2500 power operational amplifier (RCA, Somerville, NJ). Although with this setup the speaker could move as much as 150 μm in 150 μs, the largest displacement applied to the fiber was more typically 30 μm in 150 μs.

Sarcomere Length Detection. The sarcomere length detecting system consisted of a 10 mW 633 nm HeNe laser (Jodon Engineering, Ann Arbor, MI), three cylindrical focusing lenses, and a Schottky barrier position sensitive light detector (SC-10, United Detector Technology, Santa Monica, CA). The components were aligned in such a way that, with the fiber in place and illuminated, either the right or left first order diffraction line fell upon the center of the Schottky barrier photodetector. Defining the x axis as the axis of the horizontal muscle, the y axis as the axis of the horizontal laser beam, the z axis as the vertical axis, and $y = 0$ as the location of the fiber, a 200-mm focal length cylindrical lens at $y = -335$ mm compressed the beam in the z-direction and a 300-mm focal length cylindrical lens at $y = -110$ mm compressed the beam in the x-direction. This lens system caused the 1.2-mm laser beam to measure, at the plane of the fiber, ~0.25 mm in the z-direction and 0.3 mm in the x-direction. A 30-mm focal length cylindrical lens at $y = +55$ mm compressed the first order diffraction line in the z-direction onto the photodetector located at $y = +120$ mm.

Changes in position of the first order diffraction line were detected by using three terminals of the Schottky barrier photodetector. The p-terminal was reverse-biased by 15 V and the two n-terminals, which carried the currents collected at opposite ends of the detector active area, were connected to two AD511's (Analog Devices, Norwood, MA) wired in a current-to-voltage converting configuration. Each feedback loop of the AD511's had a 100 kOhm resistor and 47 pF capacitor in parallel. In addition, each AD511 had circuitry for subtracting out the dark and background currents collected at each terminal. After background current cancellation, the signals from the AD511's were electronically subtracted to produce a signal proportional to the position of the centroid of the incident light and to intensity. When the difference signal from the AD511's was divided by the sum of two signals using an AD463B divider (Analog Devices, Norwood, MA), a signal proportional only to position was generated. A 44% decrease in light intensity produced a spurious length signal of <1 nm/half-sarcomere. The detector was positioned so that the incident light fell close to the center of the active area. This minimized the sensitivity of the detector to movements of light in a direction perpendicular to the one being sensed. With this precaution, a 1-mm motion in the z-direction produced <1/20 the signal of a 1-mm motion in the x-direction.

The noise in the sarcomere length detection system depended upon the incident light intensity. With the intensity usually available from focusing the first order diffraction line from a single fiber, the noise of the sarcomere length detector was <0.1 nm/half-sarcomere. With a fiber in place, mechanical vibrations in the system raised the noise level to ~0.3 nm/half-sarcomere. A sarcomere length change of 1 nm/half-sarcomere produced a signal of 25 mV. The measured half-time for the response of the sarcomere length detector was 9 μs.

Setting up the Fiber. Since the displacement generator, fiber, and force transducer were mounted on a Unislide translation device (Velmex, East Bloomfield, NY) which was positioned on a rotary table, they could be translated, as well as rotated, relative to the laser beam. The amount of translation was measured with a noncontact eddy current displacement sensor (KD-2310-15U, Kaman Instrument Corp., Colorado Springs, CO). The amount of rotation was measured from the resistance of a 1-turn potentiometer. A 50-mm diameter wheel, attached to the shaft of the potentiometer, rubbed along the edge of the rotary table and rotated as it rotated.

After the fiber was mounted, it was translated so that the laser beam for measuring changes in sarcomere length shined on the fiber 0.5 – 1 mm from the force transducer end. The exact spot was chosen to be just beyond the region of fiber affected by gluing to the transducer. Recording the sarcomere displacement near the force transducer permitted determination of the fiber's force-displacement relationship with a minimum of artifact related to series compliance or the finite time required for mechanical signals to propagate along the length of the fiber (Schoenberg et al., 1974).

Once the fiber was axially positioned, it was then rotated relative to the laser beam so as to maximize the intensity of the first order diffraction line. This not only maximized the light signal, it enabled us to sample from the largest subpopulation of myofibrils in the event that all myofibrils were not identical (Rüdel and Zite-Ferenczy, 1979; Brenner, 1985; Sundell et al., 1986).

Measuring Chord Stiffness as a Function of Stretch Duration. Chord stiffness is defined as the force generated by a given duration stretch divided by the size of the stretch. In obtaining the relationship between chord stiffness and the duration of stretch, the force

and sarcomere length signals caused by the stretch were fed into two channels of a digital storage oscilloscope (Model 4094, Nicolet Instrument Corp., Madison, WI). To reduce noise, for each duration stretch, from 10–50 repeat traces were averaged. The multiple traces were obtained at a repeat interval of 3 s, unless the stretch duration exceeded 300 ms, in which case, the repeat interval was 10 times the stretch duration. Typically, after averaging, the noise in the traces was <0.05 nm/half-sarcomere and 0.05 dyn. After the averaged traces were collected, they were transmitted, via an RS-232 interface, to a Masscomp 68010-based supermicrocomputer (Model 5500, Masscomp, Maynard, MA).

The first step of the data analysis was to correct the force signal for the finite frequency response of the force transducer. This was done using the procedure outlined in Appendix B of Ford et al. (1977). Fig. 1 shows several typical averaged traces for three different velocity stretches applied to a single, skinned, relaxed rabbit psoas fiber, at 5°C, bathed in a solution having a total ionic strength of ~20 mM. For the fastest stretch applied, the figure shows both the original and corrected force signals. It is seen that because of the high natural frequency of the force transducer, the magnitude of the force correction is small.

From records like those shown in Fig. 1, chord stiffness was measured for stretch distances of 0.5, 1, 2, and 4 nm/half-sarcomere. This was done by having the computer analyze the time it took to stretch the fiber each distance, having it calculate the amount of force generated at the precise instant the fiber had been stretched by that distance, and having it divide the force generated by the distance stretched. The total processing, including display of the force-displacement relationship, took ~2 min, during which time the next averaged record, obtained with a different speed of stretch, could be recorded. In this way, four full chord stiffness—duration of stretch relationships, one for each chord distance, were relatively quickly obtained.

RESULTS

One important conclusion that comes from examining the thermodynamics of rapid-equilibrium crossbridges (Schoenberg, 1985) is that the horizontal position of the chord stiffness – log (duration of stretch) relationship should depend upon the crossbridge detachment rate constants. An important test of this is whether the horizontal position of the S_c – log t_d relationship indeed shifts under conditions where the detachment rate constants change. Fig. 2 shows the S_c – log t_d relationships for a fiber bathed in 2 mM Mg-adenyl-5′-yl imidodiphosphate (MgAMP-PNP) and in 2 mM magnesium pyrophosphate ($MgPP_i$).

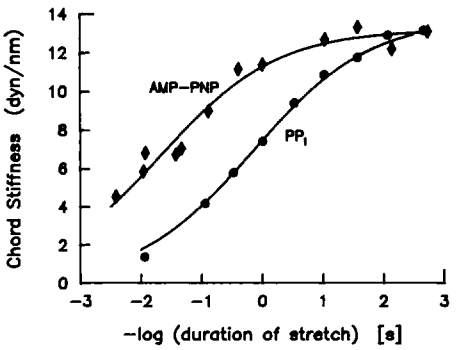

FIGURE 2 Chord stiffness versus logarithm of duration of stretch for a single skinned rabbit psoas fiber bathed in 2 mM MgAMP-PNP or 2 mM $MgPP_i$ solution. Other ionic constituents: Imidazole, 10 mM; EGTA, 3 mM; $MgCl_2$ added in excess of PP_i or AMP-PNP, 2 mM; KPropionate, 70 mM; DTT, 0.5 mM; pH = 7.0; T = 5°C. The chord distance was 2 nm/half-sarcomere. In this and subsequent figures, chord stiffness, S_c, is always plotted versus ($-\log t_d$) in order that speed of stretch increase to the right. Experiment 070787: Fiber cross-section, 107 × 107 μm; P_o = 94 dyn. A second experiment on one other fiber gave similar results. As mentioned in the text, scatter on the order of 10% for measurements made in the presence of nucleotide analogues was not uncommon. For this reason, in this figure only, the $MgPP_i$ stiffness was multiplied by 0.9 in order to make it, as seen previously on average, equal to the MgAMP-PNP stiffness for $t_d = 10^{-3}$ s.

The S_c – log t_d relationships are precisely of the type expected for an equilibrium population of crossbridges with continual crossbridge attachment and detachment. With short-duration, high-speed stretches the chord stiffness is high; with slower, longer-duration stretches the chord stiffness is considerably reduced. In solution (Roger Goody, personal communication; Jose Biosca and Evan Eisenberg, personal communication), replacing AMP-PNP with PP_i causes ~a 10 – 20 fold increase in the rate of myosin subfragment-1 (S1) detachment from actin. As Fig. 2 shows, in the fiber this causes a horizontal shift of the S_c – log t_d relationship just a little over a decade to the right. This is precisely the result expected from the '85 modeling. However, while Fig. 2 nicely illustrates the '85 theory, it is not a perfect confirmation of it since replacing

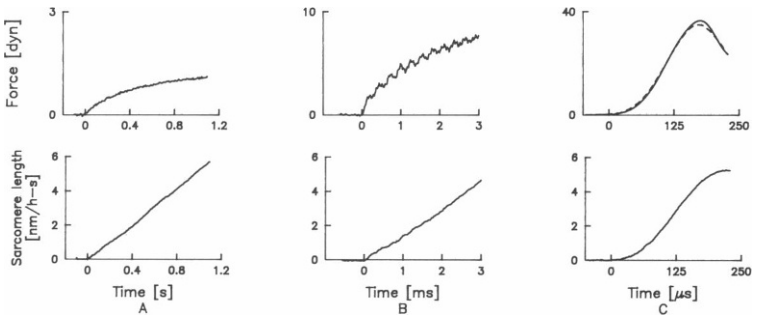

FIGURE 1 Typical sarcomere length and force traces from a single relaxed skinned rabbit psoas fiber stretched in μ = 20 mM ionic strength relaxing solution, with different velocity stretches. *A* is the slowest speed stretch, *C* the fastest. Note different time scales and force sensitivities. The dashed curve in the force panel of *C* shows the force trace corrected for the finite frequency response of the transducer according to the procedure of Ford et al., 1977. This particular force transducer had a natural period of 60 μs and a damping time constant of ~450 μs. Note that the correction is quite small, even for this transducer, the slowest one used. Experiment 092286: Fiber cross-section, 67 × 107 μm; P_o, the isometric tension measured at 5°C in μ = 170 mM contracting solution (see Schoenberg and Eisenberg, 1985), was 67 dyn.

AMP-PNP with PP_i in solution affects the S1 attachment rate constants just about as much as it does the detachment ones.

In theory, chord stiffness can depend not only upon the crossbridge detachment rate constants and the duration of stretch, but also upon the stretch amplitude (Schoenberg, 1985). Fig. 3 *A* shows the cord stiffness – log t_d relationships of a relaxed, skinned rabbit psoas fiber, bathed in a solution with an ionic strength of 20 mM, for four stretch amplitudes, 0.5, 1, 2, and 4 nm/half-sarcomere. It is seen that the S_c – log t_d relationship is more or less independent of chord amplitude. The curves for the shorter chord distances deviate slightly leftward at intermediate speeds of stretch and slightly to the right for faster speeds. However, the observed deviations are small and may simply reflect systematic reading errors caused by a small spurious 275-μs period oscillation in the original records (see Fig. 1 *B*). Most of the subsequent figures display the 4-nm/half-sarcomere chord stiffness since, in theory, this is the one least susceptible to any errors arising from uncertainties in estimation of the exact time of the start of stretch, water waves set up by the rapid speaker motion, electrical noise in the transducer traces caused by the large current driving the speaker, and residual transmission time effects. Fig. 3 *B* shows the excellent reproducibility of such data.

Having seen that it is possible to obtain a precise S_c – log t_d relationship and also that the horizontal position of the curve should give us information about the crossbridge detachment rate constants, we are now in a position to examine the influence of ionic strength on the S_c – log t_d relationship of relaxed rabbit psoas fibers. Single fibers were isolated and mounted as described in the Methods section. They were then bathed in either low ionic strength relaxing solution (μ = 20 mM) or in low ionic strength relaxing solution with 20, 60, or 140 mM added KPropionate. An S_c – log t_d relationship for stretch durations between 10^{-4} and 1 s was determined for the fiber in each of the solutions. As a reference, the rigor stiffness, which was more or less independent of stretch duration between 10^{-3} and 1 s, was also measured. Fig. 4 shows the data.

It is seen that as ionic strength increases, there is a big decrease in the chord stiffness for a given duration of

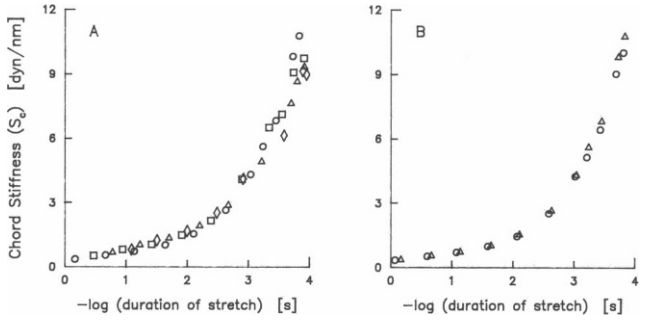

FIGURE 3. Chord stiffness versus logarithm of duration of stretch for a skinned rabbit psoas fiber bathed in 20 mM ionic strength relaxing solution. (*A*) Chord stiffness measured with different chord distances. (*B*) Reproducibility of the 4-nm/half-sarcomere chord stiffness. In *A*, chord distances, in nm/half-sarcomere, were 0.5 (◇), 1 (△), 2 (□), and 4, (○). In *B*, (○) is the low ionic strength 4-nm/half-sarcomere relationship recorded at start of experiment; (△) is the same relationship recorded some 5 h, 500–1,000 stretches, and 6 solution changes later. Experiment 043087: Fiber cross-section, 73 × 102 μm. P_o not measured. Experiments on five additional fibers gave similar results.

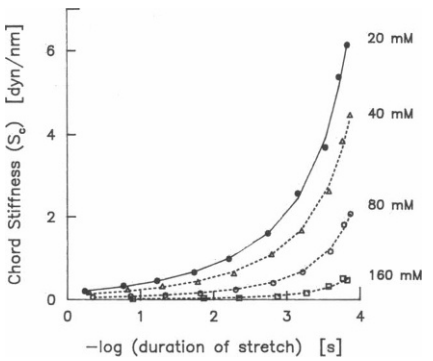

FIGURE 4 Chord stiffness versus duration of stretch for single relaxed skinned rabbit psoas fibers in solutions of different ionic strength. T = 5°C, 4 nm/half-sarcomere chord distance. The ionic strength value is given next to each curve. The significance of the solid and dashed curves is given in the legend to Fig. 5. Experiment 052086: Fiber cross-section, 78 × 97 μm. P_o = 63 dyn.

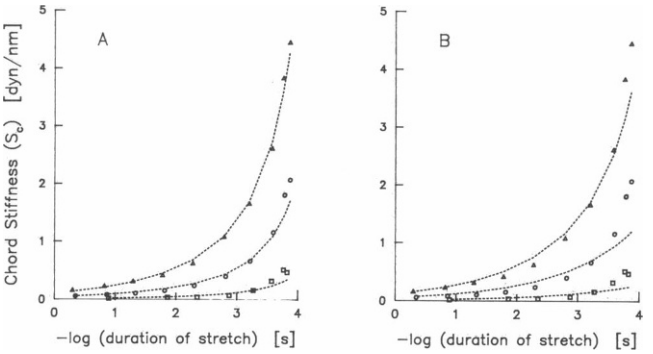

FIGURE 5. Fitting of the higher ionic strength S_c – log t_d data assuming either (*A*), that ionic strength affects only the attachment rate constants, or (*B*), that ionic stength affects only the detachment rate constants. Symbols (△, ○, □), are data obtained at ionic strengths of 40, 80, and 160 mM respectively. The dotted curves show the S_c – log t_d curves expected with either of the assumptions above. It is seen that assumption *B* is a rather poor one. The dotted curves were obtained as follows: First the μ = 20 mM ionic strength data were fitted to a sum of 2 or 3 exponentials (solid curve, Fig. 4). Expressing the relationship describing the μ = 20 mM data as $S_c = f(\log t_d)$, the dotted curves were obtained by fitting the higher ionic strength data to the relationship, $S_c = a_0 f(\log [t_d] - a_1)$, where a_1 was fixed at 0 for *A* and a_0 was fixed at 1.0 for *B*. The absolute best fit to the data, obtained by allowing both a_0 and a_1 to vary, is shown by the dotted curves in Fig. 4. In all cases the fitting was done with a nonlinear least squares alogrithm based upon Marquardt's compromise. To avoid overweighting points at either end of the scale, instead of using S_c and t_d as the fitted variables, the log of S_c was fitted to log a_0 + log f(log $[t_d]$ – a_1). The amount of shifting or scaling was directly determined from a_0 and a_1. The 95% confidence limit of the determined parameters was typically 10–25%. The average parameter values and S.E.M.'s for five complete experiments on rabbit psoas fibers are shown in Fig. 6.

stretch. It is important to know whether this decrease in chord stiffness is due to a real decrease in the number of attached crossbridges or whether, alternatively, it is due to an increase in the detachment rate constants without a change in crossbridge number. The latter might possibly occur if detachment became so rapid that our finite speed apparatus was no longer capable of detecting the attached crossbridges (Brenner et al., 1986). From the arguments in the Theory section (see also Schoenberg, 1985), we see that if increasing ionic strength is decreasing the number of attached crossbridges without affecting the detachment rate constants, it will simply cause vertical scaling of the S_c – log t_d relationship. If it is increasing the detachment rate constants without decreasing the number of attached crossbridges, it will cause the S_c – log t_d relationship to shift to the right horizontally. Fig. 5 shows an attempt to fit the data with one or the other of these two extreme possibilities. Fig. 5 *B* shows it is not at all possible to fit the data with the assumption that increasing ionic strength simply causes a big increase in the detachment rate constants. This is seen from the big divergences between data and fit for $t_d < 10^{-3}$ s and the smaller but nonetheless significant deviations for $10^{-3} < t_d < 10^{-1}$ s. In contrast, Fig. 5 *A* shows that the assumption that increasing ionic strength affects only the attachment rate constants is a reasonable one. The best fit to the data, that shown by the dotted lines in Fig. 4, suggests that as ionic strength is increased from very low values up to physiological values there is actually a very small decrease, ~two–threefold, in the detachment rate constants, with a big decrease, ~100-fold, in the attachment rate constants (see Discussion).

The complete analysis illustrated in Figs. 4–5 was repeated on five separate fibers. Fig. 6 shows the averaged results, Fig. 6 *A* showing the relative number of attached crossbridges (determined from the degree of vertical scaling) and 6 *B* showing the change in detachment rate constant (determined from the amount of horizontal shift) as ionic strength is increased from 20 up to 160 mM. We will see later that at μ = 20 mM the crossbridge detachment rate constants are in the neighborhood of 10^4 s^{-1} and the crossbridges spend ~⅔ of the time attached to actin. The data suggest that at the same time that increasing ionic strength from very low values up to physiological values by adding KPropionate causes only a small decrease, two–threefold, in the crossbridge detachment rate constants, it appears to cause a big decrease, ~20-fold in the amount of time the crossbridges spend attached to the actin filament.

One problem in calculating the relative fraction of time crossbridges spend attached to the actin filament simply by comparing the μ = 20 mM and μ = 160 mM stiffnesses is that the interfilament spacing of a relaxed skinned fiber at μ = 160 mM is considerably swollen relative to that at μ = 20 mM (Brenner et al., 1984). This must be taken into account because resting stiffness has been shown to depend upon interfilament spacing (Berman and Maughan, 1982; Goldman and Simmons, 1986). One way of decreasing the interfilament spacing of a relaxed fiber at normal ionic strength to approximately the spacing at μ = 20 mM is by adding 3% of the high molecular weight polymer Dextran T500 to the bathing solution (see Godt and Maughan, 1977; Brenner, et al., 1984). The effect this has on the resting chord stiffness is shown in Figs. 7 *A* and *B*. Fig. 7 *A* shows that adding 3% Dextran T500 to a relaxed rabbit psoas fiber at physiological ionic strength increases the resting chord stiffness ~twofold. In a total of three experiments, the average increase was 120 ± 10%. It is interesting that adding 3% Dextran T500 has little effect on the μ = 20 mM chord stiffness (Fig. 7 *B*, average ratio from three experiments, 1.07 ± 0.03). It also has little effect on

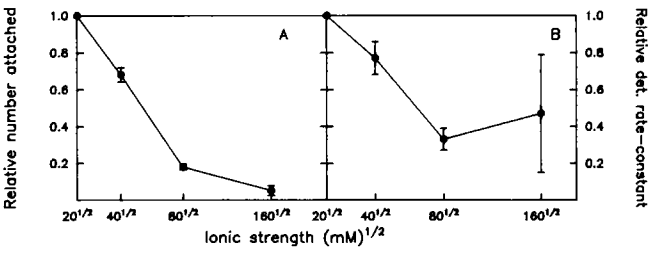

FIGURE 6 Summary of the calculated change in the fraction of attached crossbridges (*A*) and the crossbridge detachment rate constants (*B*) with increasing ionic strength. Average of five fibers. Error bars show S.E.M. At μ = 20 mM, the best estimate of the absolute fraction of attached crossbridges (equal to the fraction of time an individual crossbridge spends attached to actin) is 70 ± 20% (see Discussion). The crossbridge detachment rate constants at μ = 20 mM are ~10^4 s^{-1} (see Discussion). The data displayed are the data uncorrected for interfilament spacing changes. Correction for interfilament spacing changes would make the relative number of attached crossbridges at μ = 160 mM increase 2.2-fold (see Text and Fig. 7).

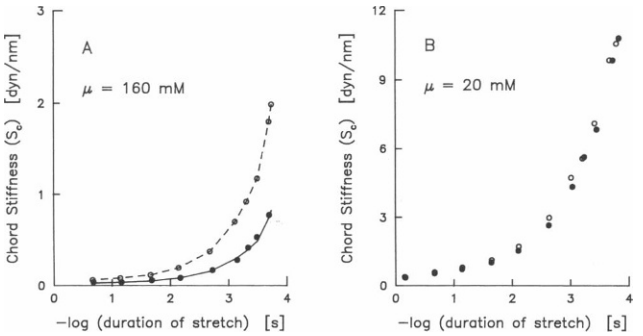

FIGURE 7. Effect of 3% Dextran T500 on the resting chord stiffness-duration of stretch relationship. (●) standard solutions; (○) standard solution plus 3% Dextran T500. (*A*), ionic strength = 160 mM; (*B*), ionic strength = 20 mM. The two curves in *A* show almost perfect scaling, the dashed curve being equal to the solid curve ×2.4. In a total of three experiments, the average scaling was 2.2 ± 0.1. Experiment 043087: Fiber cross-section, 73 × 102; P_o not measured. From the data of Brenner et al., 1984, the interfilament spacing of a relaxed fiber at μ = 160 mM with 3% Dextran is estimated to be about the same as that of the relaxed fiber at μ = 20 mM without Dextran.

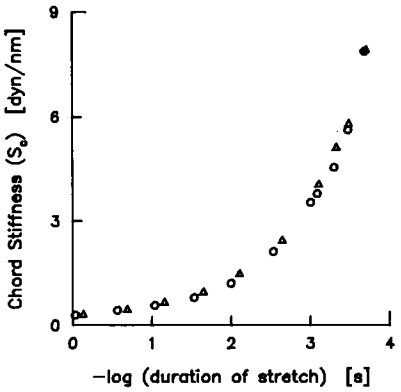

FIGURE 8 The resting chord stiffness-duration of stretch relationship at two different ATP concentrations. (O) ATP = 1 mM; (△) ATP - 0.25 mM. The 1 mM ATP solution was our standard solution; the 0.25 mM ATP solution had 0.75 mM MgATP replaced with 5 mM KPropionate. T =4.8°C. Experiment 110387: Fiber cross-section, 73 × 107 μm; P_o = 79 dyn. Experiments on three additional fibers gave similar results.

the rigor stiffness (data not shown). Thus, when interfilament spacing changes are compensated for, there is ~ a 10-fold, rather than a 20-fold, reduction in the amount of time the crossbridges spend attached to actin at normal salt compared with low salt.

It was important in our experiments to be certain we were looking at the behavior of the M · ATP crossbridge and not that of a partial rigor crossbridge. Fig. 8 shows the S_c – log t_d relationship obtained from a fiber bathed in our standard low ionic strength relaxing solution (having [ATP] = 1 mM) and the same relationship obtained from the same fiber bathed in a 20 mM ionic strength relaxing solution having an ATP concentration of 0.25 mM. It is seen that the two curves are identical. Additionally, the S_c – log t_d relationship obtained in a 40 mM ionic strength relaxing solution having a MgATP concentration of 5 mM was similar to that obtained in our standard, 1 mM MgATP, μ = 40 mM relaxing solution (data not shown). Thus the S_c – log t_d relationship is insensitive to [ATP] in the mM range and all the crossbridges presumably have MgATP (or MgADP · P_i) at the nucleotide binding site.

The question arises, particularly at physiological ionic strength, as to how much of the resting rapid chord stiffness could be due, not to the stiffness of crossbridges, but to the stiffness of the passive structures that contribute to the muscle's resting tension. To help answer this question, we performed several experiments comparing the fiber response in our standard μ = 160 mM relaxing solution with the response of the fiber in a similar solution having 140 mM KCl instead of 140 mM KPropionate. In solution (L. E. Greene, unpublished data), replacing this amount of propionate with chloride causes the binding constant of myosin subfragment-1 to actin to decrease ~ two–threefold. In the fiber, as shown in Fig. 9, this replacement has almost no effect on the resting tension, but, as shown in Fig. 10, it reduces the fibers resting rapid chord stiffness ~ twofold. This suggests that at normal

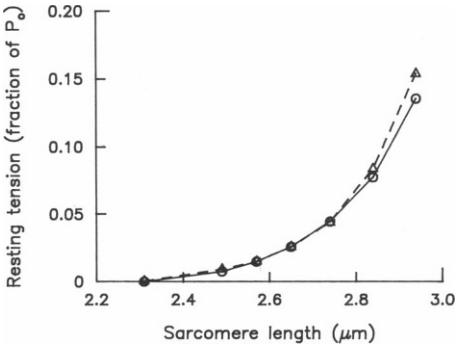

FIGURE 9 Effect of replacing 140 mM KPropionate with KCl on the resting tension of skinned rabbit psoas fibers at normal ionic strength. Circles (O), resting tension in our standard μ = 160 mM ionic strength relaxing solution. Triangles (△), resting tension measured on same fiber with 140 mM KCl replacing 140 mM KPropionate. The fiber was initially placed in propionate solution and buckled at a sarcomere length <2.3 μm to determine the zero of force. It was then adjusted to sarcomere length 2.49 μm, and subsequently stretched to sarcomere length 2.94 μm by stretching in increments of ~0.1 μm every 5 min. The tension at the end of each 5 min interval was noted. Once the fiber was stretched to 2.94 μm, the procedure was reversed, and the tensions again noted. After the fiber became buckled, the propionate solution was replaced with one containing chloride, and the stretch and release cycle repeated. There was no significant difference between the resting tension measured while increasing sarcomere length and that measured while decreasing sarcomere length. Each point represents the average of four resting tension measurements from two up-down-change solution cycles. Repeating the experiment on a second fiber, reversing the order of chloride and propionate exposure, produced a similar result. Note that the resting tension is virtually unchanged, or possibly even slightly higher, in chloride relaxing solution compared with propionate solution. Experiment 102087: Fiber cross-section, 92 × 126 μm; P_o = 78 dyn. In this experiment only, a carbon fiber extension was epoxied to the force transducer in order to give it a resolution <0.1 dyn.

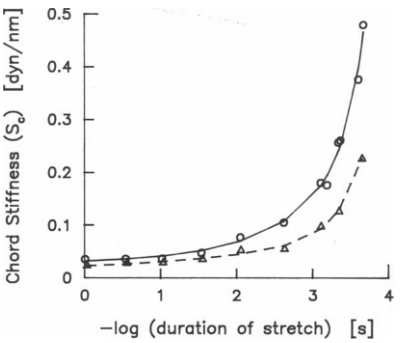

FIGURE 10 Effect of replacing 140 mM KPropionate with 140 mM KCl on the chord stiffness-duration of stretch relationship in skinned rabbit psoas fibers at normal ionic strength. Solid curve (O), S_c – log t_d relationship in our standard μ = 160 mM KPropionate solution. Dashed curve (△), S_c – log t_d relationship in same fiber after KPropionate was replaced with KCl. Experiment 102987: Fiber cross-section, 92 × 107 μm; P_o = 92 dyn. Sarcomere length. 2.5 μm. The effect was reversible and two additional experiments gave similar results.

sarcomere length (~2.5 μm in the rabbit) a good fraction of the resting chord stiffness measured in response to rapid stretches is due to crossbridges, not to the structures causing the fiber's resting tension (see also Discussion).

All the above data are from skinned rabbit psoas fibers at 5°C. The resting stiffness of single, skinned, frog semitendinosus fibers was also examined and typical S_c – log t_d plots at different ionic strengths are shown in Fig. 11. Again we see the kind of speed dependence of chord stiffness that is characteristic of rapid-equilibrium crossbridges. However, normalized either to rigor stiffness or cross-sectional area, in the frog, the chord stiffness at a given ionic strength and speed of stretch is two to three times lower than in the rabbit. In rabbit, the stiffness measured at μ = 20 mM with our fastest stretch was 51 ± 3% of the rigor stiffness (n = 8). In frog, (n = 5), the corresponding number was 28 ± 7%. Normalized to cross-sectional area, the maximum μ = 20 mM resting stiffness in the rabbit was 1.17 ± 0.14 × 10^{-3} dyn/(nm/half-sarcomere)/(μm)^2 (n = 7) and in the frog, (n = 5), it was 0.386 ± 0.13 × 10^{-3} dyn/(nm/half-sarcomere)/(μm)^2. The data from frog, obtained over two different seasons, seemed somewhat more variable than that from rabbit. Larger fibers, as noted before by Ford et al., 1977, tended to have significantly less resting stiffness per cross-sectional area. It is possible this might represent a true dependence of the frog's resting stiffness on season, fiber type, or diameter, but it was not possible to ascertain this with the limited number of fibers studied.

DISCUSSION

General

A significant advance in understanding muscle behavior has been the realization that, in many regards, the muscle proteins in the fiber behave like proteins in solution. It is now quite clear that, just as for noncovalent binding of proteins in solution, when we speak of the crossbridges as being bound to actin, we mean not that they are immutably fixed to the actin filament, but only that the attachment and detachment rate-constants are such so as to favor attachment over detachment. Even under conditions where the equilibrium is well shifted towards attachment (such as crossbridge binding to actin in the presence of $MgPP_i$ or MgAMP-PNP at moderate or low ionic strength) the myosin crossbridges continually detach from and rebind to the actin filament (see Fig. 2; also Schoenberg and Eisenberg, 1985).

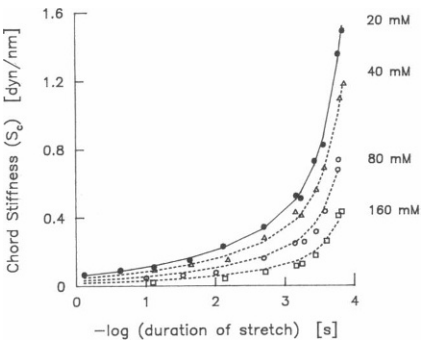

FIGURE 11 Chord stiffness versus duration of stretch for a single frog semitendinosus fiber. Conditions like Fig. 4, except T = 4°C, sarcomere length = 2.4 μm. Experiment 091486: Fiber cross-section, 87 × 97 μm, P_o = 138 dyn. Two additional complete experiments on frog fibers gave similar results. Figure reprinted with permission from Schoenberg, 1988.

In a fiber, when a crossbridge detaches from a site on the actin filament, it need not necessarily reattach back to the same site. When the crossbridges have been strained by stretch of the fiber, the detaching crossbridges will tend to reattach back to actin sites in positions of lesser strain. If the stretch can be completed on a time scale short compared with the crossbridge detachment rate constants, one may determine the detachment rate constants simply from the rate at which the force generated by the stretch decays. We used this technique before to study crossbridges having either MgAMP-PNP or $MgPP_i$ at the active nucleotide binding site, finding that the detachment rate constants in the presence of PP_i are ~15 times faster than in the presence of AMP-PNP (Schoenberg and Eisenberg, 1985). However, this technique cannot be applied to crossbridges having ATP at the nucleotide binding site because with ATP, the crossbridges detach on a time scale too fast for the fiber stretch to be completed.

An alternative method developed for obtaining the crossbridge detachment rate constants involves measuring the chord stiffness of a fiber with different duration ramp stretches (Schoenberg, 1985). Since the chord stiffness will be maximal when measured with a stretch duration too short to allow any crossbridge detachment and very small when measured with a stretch duration that allows multiple detachment and reattachment, the horizontal position of a plot of chord stiffness versus the logarithm of the stretch duration will provide information about the crossbridge detachment rate constants. We saw this illustrated in Fig. 2 and in the present study, this technique was applied to study the relaxed crossbridge.

It was possible, in resting rabbit psoas fibers, to make accurate and quite reproducible measurements of the chord stiffness-duration of stretch relationship. It was not clear that this would necessarily be the case since our method rests heavily on the use of laser diffraction, a technique known to be fraught with difficulty (Rüdel and Zite-Ferenczy, 1979). The excellent reproducibility of our resting S_c – log t_d curves (Fig. 3 B) is undoubtedly related to the fact that our measurements of sarcomere length changes during stretch were both reproducible and also insensitive to small variations in either angle or horizontal position of the laser beam (see Brenner, et al., 1986).

The reproducibility of data from relaxed frog semitendinosus fibers was nearly as good as illustrated in Fig. 3 B, but that from rabbit and frog rigor fibers was not. The best rabbit rigor fibers behaved reproducibly to within a few

percent but fibers showing scatter on the order of 10 or occasionally even 20% were not uncommon. The difference in precision of measurements on relaxed fibers compared with rigor fibers may be related to differences in distortion of the orientation of the myofibrils with stretch. Thus, possibly in the rigor case, larger changes in the angular orientation of the myofibrils with stretch may amplify artifacts related to Bragg angle effects (Rüdel and Zite-Ferenczy, 1979; Goldman, 1987).

The Fiber Rate and Binding Constants

From our results, it is possible to make reasonable estimates of the detachment rate constants, and also the fiber binding constants. From these, indirectly the attachment rate constants of the M · ATP crossbridge may also be evaluated. The detachment rate constants are obtained by fitting the data of Fig. 4 to either Eq. 1 or 2. Fig. 12 *A* shows μ = 20 mM the fitted data to Eq. 1. The fact that the theoretical one-rate constant curve is steeper than the data suggests that the M · ATP crossbridge does not detach with a single rate constant but with a somewhat wider range of rate constants (see Schoenberg, 1985). We can estimate what this range is by fitting the data to Eq. 2 using two or more rate constants. The 3-rate constant fit is shown in Fig. 12 *B*. While the assumption that 100% of the crossbridges detach with a single rate constant does not give an exceptionally good fit to the data (Fig. 12 *A*), the best 3-exponential fit (Fig. 12 *B*), which fits the data nearly perfectly, has ~90% of the crossbridges detaching with only one of the rate constants. This situation, which was seen for all five experiments analyzed in detail, is quite different from what is seen for crossbridges with MgAMP-PNP or $MgPP_i$ at the active site. With AMP-PNP or $MgPP_i$, a 3-exponential fit gives three equally-weighted rate constants, the fastest and slowest separated by almost three decades (Schoenberg and Eisenberg, 1985). Since the single-exponential fit for the M · ATP crossbridge at very low ionic strength gives a detachment rate constant of 4×10^3 s^{-1}, while the 3-exponential fit has 90% of the crossbridges detaching with a rate constant of $\sim 2 \times 10^4$ s^{-1}, it is clear that in contrast to the behavior of the M · AMP-PNP or M · PP_i crossbridge, the majority of the M · ATP crossbridges detach, at low ionic strength, over a narrow range of rate constants centered in the neighborhood of 10^4 s^{-1}.

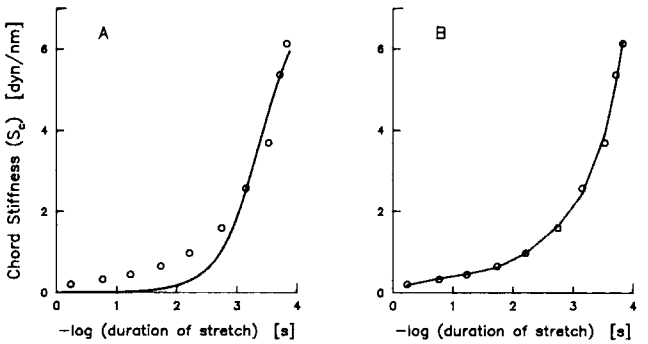

FIGURE 12 Fitting the chord stiffness-duration of stretch relationship of a relaxed skinned rabbit psoas fiber in 20 mM ionic strength relaxing solution either (*A*), to Eq. 1, or (*B*), Eq. 2. Open circles, data; solid lines, fitted curves. For solid line in *A*, n = 1.0, $k_1 = 4.1 \times 10^3$ s^{-1}. In (*B*), n_1 = 0.91, $k_1 = 2.3 \times 10^4$ s^{-1}, n_2 = 0.06, k_2 = 390 s^{-1}, n_3 = 0.03, k_3 = 3.7 s^{-1}. Same fiber as Fig. 4. For the five rabbit fibers summarized in Fig. 6, n_1 averaged 0.88 +/− 0.02 and k_1 averaged (1.74 +/− 0.20) $\times 10^4$ s^{-1}.

The detachment rate constants at normal ionic strength are somewhat more difficult to estimate since the substantially lower amplitude of the μ = 160 mM data makes the procedure outlined above less reliable. Another way of approaching the problem is to use the low ionic strength data as a reference condition and consider the relative effect of increasing ionic strength. To do this, we make use of the finding discussed above that the horizontal position of the S_c − log t_d relationship is determined mainly by the crossbridge detachment rate constants. A maneuver such as increasing ionic strength, if it affects the detachment rate constants, should cause a horizontal shift in the S_c − log t_d curve. If changing ionic strength affects the number of attached crossbridges without affecting the detachment rate constants, i.e., if it affects only the attachment rate constants, it should simply cause the S_c − log t_d curve to scale. As we saw from Fig. 5 *A*, the attempt to fit the ionic strength data for the rabbit assuming only scaling gives a fairly reasonable fit. However, the fact that the actual data are slightly more concave upward than the scaled curves suggests that, in addition to causing scaling, increasing ionic strength also causes a slight leftward shift in the S_c − log t_d curve. It was found, doing a best least-squares fit to the data, that increasing ionic strength from μ = 20 mM to μ = 160 mM causes a shift in the S_c − log t_d relationship of ~0.33 ± 0.30 decades to the left. This corresponds to only ~ a 2.1 ± 1.4-fold decrease in the crossbridge detachment rate constants (see Fig. 6 *B*). The corresponding decrease going to 80 mM ionic strength was 3.0 ± 0.6-fold. Thus at physiological ionic strength, the detachment rate constants of the M · ATP crossbridge are on the order of 3×10^3 to 10^4 s^{-1}.

The attachment rate constants must be deduced in a somewhat less direct fashion. Since the attachment rate constants do not greatly influence the S_c − log t_d relationship except as they modulate the number of crossbridges attached, it is necessary first to estimate the latter in order to know the former (see Eqs. 1 and 2; also Schoenberg, 1985). Although we do not know for sure the exact number of attached M · ATP crossbridges in a relaxed rabbit psoas fiber, there is now quite a bit of information concerning this. This information may be summarized as follows: (*a*) X-ray diffraction studies that attempt to estimate the number of crossbridges attached by estimating the amount of mass in the vicinity of the thin filaments (L. C. Yu and B. Brenner, manuscript in preparation) estimate that between 60 and 80% of the crossbridges are attached at very low ionic strength. (*b*) Stiffness measurements such as

those reported here show that the stiffness in low ionic strength relaxing solution, measured with the fastest stretches is just over 50% of the rigor stiffness (see also Brenner et al., 1982, 1986). Since it is possible that the maximum chord stiffness measured in the relaxed fiber might be higher if we could stretch faster, if we assume that the stiffness per bridge is the same in a relaxed fiber as it is in rigor, and that all the bridges are attached in rigor (Lovell and Harrington, 1981; Cooke and Franks, 1980; Cooke and Thomas, 1980), then 50% becomes a reasonable lower estimate of the number of crossbridges attached in μ = 20 mM relaxing solution. The binding constant of the M · ATP crossbridge at low ionic strength must therefore be >1. (*c*) Causing a slight weakening of the binding constant at low ionic strength by increasing the ionic strength only slightly results in a significant decrease in the number of crossbridges attached. The binding constant at low ionic strength must therefore be <10, because otherwise a small decrease in its value would not cause crossbridge detachment. (*d*) When the crossbridge binding constant is substantially weakened by the addition of 140 mM KPropionate to very low ionic strength relaxing solution, there is ~ a 10-fold decrease in the number of attached crossbridges.

Since these observations argue that the crossbridge binding constant is between 1 and 10 at very low ionic strength, the crossbridge attachment rate constants at very low ionic strength must be 1–10 times the detachment ones. That is, they must be $\sim 10^4 - 10^5$ s^{-1}. In addition, a binding constant of 1–10 means that at low ionic strength, the M · ATP crossbridges spend 50–90% of the time attached to actin. Since our data suggest that at normal ionic strength the crossbridges spend 1/10 as much time attached to actin, at normal ionic strength the crossbridges must spend 5–9% of the time attached to actin. This means that the binding constant at normal ionic strength is in the range of 0.05-0.1 and the attachment rate constants must therefore be on the order of 100–1000 s^{-1}. The attachment and detachment rate constants of the M · ATP crossbridge for skinned rabbit psoas fibers, and also the fraction of time the crossbridges spend attached to actin in a relaxed fiber, are summarized in Table I.

For frog semitendinosus fibers, the rapid resting stiffness for a given ionic strength and duration of stretch is only ~1/2 to 1/3 that of rabbit psoas fibers. This could mean either that in the relaxed frog fewer weakly binding crossbridges are attached, or alternatively, that the same numbers are attached but the detachment rate constants are faster. The finding from the x-ray data of Xu et al. (1987) that the mass transfer at low ionic strength is significantly smaller in the frog compared with the rabbit supports the first hypothesis.

It is important to ask whether the relatively small resting chord stiffnesses measured at physiological ionic strength could be mainly due, not to rapid equilibrium crossbridges, but to the passive structural elements responsible for a muscle fiber's resting tension. Several lines of evidence suggest it is not. First of all, at the sarcomere length we work at in the rabbit, the resting tension is very, very small, ~1% of the maximum isometric tension. Secondly, although the rapid resting stiffness at normal ionic strength is also somewhat small, its stretch duration dependence is practically identical to that of the much larger, obviously crossbridge related stiffness, which is measured (Brenner et al., 1982) at low ionic strength. Thirdly, and most importantly, a strong suggestion that the rapid resting stiffness is mainly due to rapid-equilibrium crossbridges comes from the observation that when one replaces propionate with chloride, there is about a twofold decrease in the rapid resting stiffness (Fig. 10). The fact that

TABLE I
SUMMARY OF THE CROSSBRIDGE ATTACHMENT AND DETACHMENT RATE CONSTANTS OF RELAXED SKINNED RABBIT PSOAS FIBERS AT 5°C*

Parameter	Low salt (μ = 20 mM)	Normal salt (μ = 160 mM)
Detachment rate constants (s^{-1})	$\sim 10^4$	$\sim 3 \times 10^3$
	$(5 \times 10^3 - 5 \times 10^4)$‡	$(2 \times 10^3 - 2 \times 10^4)$‖
Attachment rate constants (s^{-1})	$\sim 2 \times 10^4$	~250
	$(5 \times 10^3 - 5 \times 10^5)$§§	$(100 - 1000)$§§,‡‡
Percent attached to actin	70	7
	(50 – 90)§	(5 – 9)**,‡‡

*Most likely values, with estimated range of uncertainty given below in parentheses.
‡Obtained from the horizontal position of the S_c – log t_d relationship, or equivalently, by fitting relationship to Eq. 1 or 2.
§Obtained either by assuming that the stiffness of a relaxed crossbridge is similar to that of a rigor crossbridge or from x-ray diffraction results.
‖Obtained from the horizonal shift of the S_c – log t_d relationship with increased salt.
**Obtained from the vertical scaling of the S_c – log t_d relationship with increased salt.
§§Calculated from the detachment rate constants and fraction attached according to the approximation, $n_b = f/(f + f')$, where n_b is the number of attached crossbridges and f and f' are the attachment and detachment rate constants respecively.
‡‡With interfilament spacing changes compensated for.

replacing propionate with chloride has virtually no effect on the resting tension (Fig. 9), while in solution it causes a two–threefold decrease in the binding constant of myosin subfragment-1 to actin (L. E. Greene, manuscript submitted for publication), strongly suggests the conclusion that the rapid stiffness is due mainly to crossbridges, not resting tension structures.

One may actually estimate the contribution of the resting tension structures to the rapid chord stiffness at physiological ionic strength. At a sarcomere length of 3.5 μm, where we are looking primarily at the stiffness of the structures responsible for the fiber's resting tension, the resting rapid chord stiffness is $\sim 1/10$ of the rigor stiffness measured at 2.5 μm (Brenner et al., 1982). If we assume that the component of the resting chord stiffness due to the structures responsible for the fiber's passive resting tension is proportional to the slope of the resting tension-sarcomere length relationship, then, since the slope of that relationship at 2.5 μm is $\sim 1/10$ that at 3.5 μm (Fig. 9; also Horowits and Podolsky, 1988), the contribution of the resting tension structures to the resting rapid chord stiffness at sarcomere length 2.5 μm is estimated to be $\sim 1/100$ of the rigor stiffness. Since the measured resting rapid chord stiffness under these conditions is about $1/20$ of the rigor stiffness, this suggests that the noncrossbridge contribution to the rapid resting stiffness of rabbit psoas fibers in physiological ionic strength propionate solution is probably on the order of only 1 part in 5.

Relationship to the Mechanism of Muscle Relaxation

From the data presented, it is clear that, in fully relaxed fibers, M · ATP crossbridges continually attach to and detach from the actin filament over a wide range of ionic strengths. Thus the current results strongly support our previous contention, based on our experiments at low ionic strength (Brenner et al., 1982; Schoenberg et al., 1984), that muscle relaxation cannot be due solely to troponin and tropomyosin blocking attachment as envisioned by the classic steric blocking model for muscle relaxation (Huxley, 1972, Haselgrove, 1972; Parry and Squire, 1973). Our evidence strongly suggests that blockage of a step subsequent to attachment is essential and necessary for muscle relaxation.

The finding that keeping a muscle relaxed depends upon blockage of a step subsequent to attachment raises a number of questions. The first of these concerns which step is blocked. It is clear from the work of D. K. Hill (1968), Lännergren (1971), Haugen and Sten-Knudsen (1981), our own work, and that of others, that only very few strongly-binding crossbridges exist in a relaxed fiber. Thus the step subsequent to attachment which is blocked to keep a muscle relaxed is one that prevents the weakly-binding M · ATP crossbridges from going on through the crossbridge cycle onto the more strongly-binding states.[1] Whether the step blocked is the actual force producing power stroke step, or one before it, remains to be seen. In solution, the step blocked during inhibition of the actosubfragment-1 ATPase appears to be at or near the phosphate release step (Chalovich and Eisenberg, 1982; Rosenfeld and Taylor, 1987).

Another question unanswered by the current data are whether Ca^{2+} has any effect on the binding of the M · ATP crossbridge. In solution, the biochemical evidence suggests that the effect of Ca^{2+} on the binding of subfragment 1 or heavy meromyosin to regulated actin is <5–10-fold (Chalovich and Eisenberg, 1982; Wagner and Giniger, 1981; Wagner, 1984; Chalovich and Eisenberg, 1986; Rosenfeld and Taylor, 1987). Presently, unfortunately, there is very little fiber evidence concerning this. The finding that mass shifts towards the actin filament upon activation at physiological ionic strength does not shed light on this question because it is not yet known whether any of this mass shift is due to an increase in the binding of the M · ATP crossbridge or whether most of it is due to the continually attaching and detaching M · ATP crossbridges going on through the crossbridge cycle (after attachment) to more strongly-binding states. To resolve this question, it will be necessary to develop techniques for detecting weakly-binding bridges under conditions where they coexist with more strongly-binding states.

Separate from the question of whether the troponin–tropomyosin regulatory system has much influence on the binding of the M · ATP crossbridge, another question that remains is whether the weak binding of the M · ATP crossbridge at physiological ionic strength contributes to muscle regulation. The finding that muscle fibers are perfectly well regulated at low ionic strength where the binding constant of the M · ATP crossbridge is greatly increased suggests it does not. On the other hand, the finding that fully relaxed muscle fibers at low ionic strength can become partially activated by small changes in temperature or free Mg^{+2} (Gulati, 1983) suggests that perhaps it does. Resolution of this question will clearly require a more detailed knowledge of the regulatory mechanism.

When a fiber becomes activated by Ca^{2+}, there will be a mixture of weakly- and strongly-binding crossbridge states. The overall fraction of weakly-binding crossbridge states in an activated fiber will be determined by the rate constant governing the transition from the weakly-binding to strongly-binding states and also that which governs the transition back to the weakly-binding states. The finding

[1]Calling the weakly-binding relaxed crossbridges M · ATP crossbridges is simply a matter of nomenclature and is not meant to imply that hydrolysis is the step that is blocked in relaxation; the resting crossbridges may in fact have ADP · P_i, rather than ATP, at the nucleotide binding site (Marston and Tregear, 1972).

that the stiffness of an activated fiber measured with a moderate velocity stretch is 60–80% that of a rigor fiber (M. Schoenberg, manuscript submitted for publication; Goldman and Simmons, 1977; Yamamoto and Herzig, 1978), along with the fact that nearly 100% of the crossbridges appear to be attached in rigor, suggests that in an activated fiber ~20–40% of the crossbridges are in M · ATP-like states. If Ca^{2+} has no effect on the strength of binding of the M · ATP crossbridge (Chalovich and Eisenberg, 1982), then in an activated fiber at normal ionic strength, <4% of the M · ATP-like crossbridges (10% of 40%) will actually be attached. If Ca^{2+} increases the binding of the M · ATP crossbridge 5–10-fold as more recent evidence suggests (Wagner, 1984; Chalovich and Eisenberg, 1986), then perhaps the number of weakly-binding crossbridges attached in an active fiber will be in the 10–20% range.

From the above arguments, it would appear that the attached M · ATP crossbridge state most likely is different from any of the force producing states postulated by Huxley and Simmons, 1971. Those states were postulated to be more strongly binding and also to have slower attachment and detachment rate constants. The M · ATP state may, however, be similar to the crossbridge state that was postulated by Huxley, 1972, in order to explain better the energetics of muscle contraction.

Comparison to Solution and Other Systems

The first suggestion that possibly there might be crossbridges attached in a relaxed fiber came from the biochemical studies of Chalovich et al. (1982) It is interesting how closely the behavior of the weakly-binding crossbridges in fibers actually mirrors the behavior of S1 · ATP in solution. The interaction of S1 with actin in the presence of ATP at 20°C, 0.1 M KCl, and pH 7 is described (Geeves et al., 1986) by the reaction scheme

$$\mathrm{AM} + \mathrm{T} \underset{}{\overset{K_1 = 10^3\ \mathrm{M}^{-1}}{\rightleftharpoons}} \mathrm{AMT} \underset{k_2 \sim 1\ \mathrm{s}^{-1}}{\overset{k_2 = 5{,}000\ \mathrm{s}^{-1}}{\rightleftharpoons}}$$

$$\mathrm{A\text{-}MT} \overset{k_3 > 5{,}000\ \mathrm{s}^{-1}}{\rightleftharpoons} \mathrm{A} + \mathrm{MT}$$

where AM and A-M represent two conformations of the actin myosin linkage and T represents ATP. Virtually the same scheme apparently applies to the fiber. Thus, Goldman and colleagues (Goldman et al., 1984), starting from AM and adding ATP, measured a second order rate constant for ATP binding, K_1k_2, of $\sim 10^6\ \mathrm{M}^{-1}\ \mathrm{s}^{-1}$. They further found, in agreement with a K_1 value of $10^3\ \mathrm{M}^{-1}$, that the rate of crossbridge detachment in their experiments varied with ATP concentrations up to 1 mM. In our experiments, where presumably we are starting from an A-MT -like state, we find a crossbridge detachment rate constant, k_3, of $10^4\ \mathrm{s}^{-1}$. As expected from the above scheme, this is independent of ATP concentration in the 0.25–5 mM range. Thus, both with regard to the rate constant for ATP binding, and also the rate constant for the actual detachment step, there appears to be good agreement between fiber and solution.

Another area of agreement between fiber and solution concerns the effect of ionic strength on the binding constant of the M · ATP crossbridge. We have already discussed that replacing 140 mM propionate with chloride, which in solution causes a two–threefold decrease in the binding constant of myosin subfragment-1 to regulated actin, in the fiber, causes a twofold decrease in the rapid resting stiffness. Additionally, increasing ionic strength in solution from μ = 20 to μ = 160 mM by adding 140 mM KCl causes ~ a 100-fold weakening of the binding constant of myosin subfragment-1 to unregulated actin (Greene et al., 1983). If we assume, based upon the stiffness and x-ray measurements, that ~70% of the crossbridges are attached at μ = 20 mM, then that same maneuver of adding 140 mM KCl in the fiber causes the fiber binding constant to be reduced from ~2 to ~0.03, ~ a 70-fold reduction. Thus, increasing ionic strength in the fiber, where all the regulatory proteins are present, produces about the same weakening of binding as occurs in solution in the absence of regulatory proteins. This is particularly important because it shows that even if ionic strength has some effect on the troponin–tropomyosin regulatory system, the effect is not one that greatly influences the strength of binding of the M · ATP crossbridge.

A final similarity between fiber and solution is the fact that in both cases the major effect of ionic strength is on the attachment rate constants. These similarities serve to reinforce the idea that the weakly-binding crossbridge states seen in the fiber closely resemble the weakly-binding M · ATP state seen in solution. M · ATP-like crossbridges have now been found in rabbit, frog, crab and perhaps even one type of smooth muscle (Brenner et al., 1982; Xu et al., 1987; Wakabayashi et al., 1984; K. Wakabayashi, personal communication; Siegman et al., 1976). Although the exact strength of binding may not be the same in all species (this paper, Xu et al., 1987, Brenner and Squire, 1987), none-the-less, the phenomenon of weakly-binding crossbridges, like the phenomenon of equilibrium rather than irreversible attachment, may very well be a rather general one. It is thus interesting to speculate what the role of the M · ATP crossbridge might be.

One of the great mysteries with regard to muscle contractions is how the power stroke of a 20-nm crossbridge can produce motions believed to be as large as 10 nm (Ford et al., 1977). If one assumes that only strongly-binding crossbridge states attach to actin and that these bind to actin as stereospecifically as the rigor crossbridge does, then, from a knowledge of the conformational changes in other proteins, it is hard to imagine how such large scale motions are generated. On the other hand, the configurations of S1 · ATP bound to actin, and also M · ATP crossbridges bound to actin, have been shown to

be rather nonstereospecific and quite different from the binding configuration in rigor (Craig et al., 1985; Brenner et al., 1984; Matsuda and Podolsky, 1984). With the knowledge that there are two types of attached crossbridges, it is tempting to speculate that only by having the M · ATP or a similar type crossbridge as the first attached state in the crossbridge cycle is it possible for muscle to produce the uniquely large motions that are thought to accompany the power stroke.

The author thanks the many scientists who gave him permission to reference their unpublished work. The ramp generator used in these studies to control the loudspeaker motion was fabricated by National Institutes of Health's Biomedical Engineering and Instrumentation Branch and expertly designed by Mr. Horace Cascio.

Received for publication 27 November 1987 and in final form 14 March 1988.

REFERENCES

Bagshaw, C. R., and D. R. Trentham. 1974. The characterization of myosin-product complexes and of product-release steps during the magnesium ion-dependent adenosine triphosphatase reaction. *Biochem. J.* 141:331–349.

Berman, M. R., and D. W. Maughan. 1982. Axial elastic modulus as a function of relative fiber width in relaxed skinned muscle fibers. *Pflüegers Arch. Eur. J. Physiol.*, 393:99–103.

Brenner, B. 1985. Sarcomere domain organization within single skinned rabbit psoas fibers and its effects on laser diffraction studies. *Biophys. J.* 48:967–982.

Brenner, B., J. M. Chalovich, L. E. Greene, E. Eisenberg, and M. Schoenberg. 1986. Stiffness of skinned rabbit psoas fibers in MgATP and $MgPP_i$ solution. *Biophys. J.* 50:685–691.

Brenner, B., M. Schoenberg, J. Chalovich, L. Greene, and E. Eisenberg. 1982. Evidence for crossbridge attachment in relaxed muscle at low ionic strength. *Proc. Natl. Acad. Sci. USA.* 79:7288–7291.

Brenner, B., and J. M. Squire. 1987. Rapid stiffness of single relaxed skinned fish fibres: no detectable crossbridge attachment at low ionic strength. *J. Muscle Res. Cell Motil.* 8:67.

Brenner, B., L. C. Yu, and R. J. Podolsky. 1984. X-ray evidence for crossbridge formation in relaxed muscle fibers at various ionic strengths. *Biophys. J.* 46:299–306.

Chalovich, J. M., and E. Eisenberg. 1982. Inhibition of actomyosin ATPase activity by troponin–tropomyosin without blocking the binding of myosin to actin. *J. Biol. Chem.* 252:2432–2437.

Chalovich, J. M., and E. Eisenberg. 1986. The effect of troponin–tropomyosin on the binding of heavy meromyosin to actin in the presence of ATP. *J. Biol. Chem.* 261:5088–5093.

Cooke, R., and K. Franks. 1980. All myosin heads form bonds with actin in rabbit rigor skeletal muscle. *Biochemistry.* 19:2265–2269.

Cooke, R., and D. Thomas. 1980. Spin label studies of the structure and dynamics of glycerinated muscle fibers: applications. *Fed. Proc.* 39:1962.

Craig, R., L. E. Greene, and E. Eisenberg. 1985. Structure of the actin-myosin complex in the presence of ATP. *Proc. Natl. Acad. Sci. USA.* 82:3247–3251.

Eastwood, A. B., D. S. Wood, K. L. Bock, and M. M. Sorenson. 1979. Chemically skinned mammalian skeletal muscle. 1. The structure of skinned rabbit psoas. *Tissue and Cell* 11:553–566.

Eisenberg, E., and L. E. Greene. 1980. The relation of muscle biochemistry to muscle physiology. *Annu. Rev. Physiol.* 42:293–309.

Ford, L. E., A. F. Huxley, and R. M. Simmons. 1977. Tension responses to sudden length change in stimulated frog muscle fibres near slack length. *J. Physiol. (Lond.).* 269:441–515.

Geeves, M. A., T. E. Jeffries, and N. C. Millar. 1986. ATP-induced dissociation of rabbit skeletal actomyosin subfragment. 1. Characterization of an isomerization of the ternary acto-S1-ATP complex. *Biochemistry.* 25:8454–8458.

Godt, R. E., and D. W. Maughan. 1977. Swelling of skinned muscle fibers of the frog. Experimental observations. *Biophys. J.* 19:103–116.

Goldman, Y. E. 1987. Measurement of sarcomere shortening in skinned fibers from frog muscle by white light diffraction. *Biophys. J.* 52:57–68.

Goldman, Y. E., M. G. Hibberd, and D. R. Trentham. 1984. Relaxation of rabbit psoas muscle fibres from rigor by photochemical generation of adenosine-5′-triphosphate. *J. Physiol. (Lond.).* 354:577–604.

Goldman, Y. E., and R. M. Simmons. 1977. Active and rigor muscle stiffness. *J. Physiol (Lond.).* 269:55P–57P.

Goldman, Y. E., and R. M. Simmons. 1986. The stiffness of frog skinned muscle fibres at altered lateral filament spacing. *J. Physiol. (Lond.).* 378:175–194.

Greene, L. E., and E. Eisenberg. 1980. Dissociation of the actin · subfragment 1 complex by adenyl-5′-yl imidodiphosphate, ADP, and PP_i. *J. Biol. Chem.* 255:543–548.

Greene, L. E., J. R. Sellers, E. Eisenberg, and R. S. Adelstein. 1983. Binding of gizzard smooth muscle myosin subfragment 1 to actin in the presence and absence of adenosine 5′-triphosphate. *Biochemistry.* 22:530–535.

Gulati, J. 1983. Magnesium ion-dependent contraction of skinned frog muscle fibers in calcium-free solution. *Biophys. J.* 44:113–121.

Haselgrove, J. C. 1972. X-ray evidence for a conformational change in the actin-containing filaments of vertebrate striated muscle. *Cold Spring Harbor Symp. Quant. Biol.* 37:341–352.

Haugen, P., and O. Sten-Knudsen. 1981. The dependence of the short-range elasticity on sarcomere length in resting isolated frog muscle fibres. *Acta. Physiol. Scand.* 112:113–120.

Hibberd, M. G., and D. R. Trentham. 1986. Relationships between chemical and mechanical events during muscular contraction. *Annu. Rev. Biophys. Biophys. Chem.* 15:119–161.

Highsmith, S. 1976. Interactions of the actin and nucleotide binding sites on myosin subfragment 1. *J. Biol. Chem.* 251:6170–6172.

Hill, D. K. 1968. Tension due to interaction between sliding filaments in resting striated muscle. The effect of stimulation. *J. Physiol. (Lond.).* 199:637–684.

Hodgkin, A. L., and P. Horowicz. 1960 Potassium contractures in single muscle fibres. *J. Physiol. (Lond.).* 153:386–403.

Horowits, R., and R. J. Podolsky. 1988. Thick filament movement and isometric tension in activated skeletal muscle. *Biophys. J.* 54:00–00.

Huxley, H. E. 1972. Structure changes in the actin- and myosin-containing filaments during contraction. *Cold Spring Harbor Symp. Quant. Biol.* 37:361–376.

Julian, F. J. 1971. The effect of calcium on the force-velocity relation of briefly glycerinated frog muscle fibres. *J. Physiol. (Lond.).* 218:117–145.

Lännergren, J. 1971. The effect of low-level activation on the mechanical properties of isolated frog muscle fibers. *J. Gen. Physiol. (Lond.).* 58:145–162.

Lovell, S. J., and W. F. Harrington. 1981. Measurement of the fraction of myosin heads bound to actin in rabbit skeletal myofibrils in rigor. *J. Mol. Biol.* 149:659–674.

Lymn, R. W., and E. W. Taylor. 1971. Mechanism of adenosine triphosphate hydrolysis by actomyosin. *Biochemistry.* 10:4617–4624.

Marston, S. B., and R. T. Tregear. 1972. Evidence for a complex between myosin and ADP in relaxed muscle fibres. *Nature (Lond.).* 235:23–24.

Marston, S. B., R. T. Tregear, C. D. Rodger, and M. L. Clarke. 1979. Coupling between the enzymatic site of myosin and the mechanical output of muscle. *J. Mol. Biol.* 128:111–126.

Matsuda, T., and R. J. Podolsky. 1984. X-ray evidence for two structural states of the actomyosin cross-bridge in muscle fibers. *Proc. Natl. Acad. Sci. USA.* 81:2364–2368.

Parry, D. A. P., and J. M. Squire. 1973. The structural role of

tropomyosin in muscle regulation: analysis of x-ray diffraction patterns from relaxed and contracting muscles. *J. Mol. Biol.* 75:33–55.

Rosenfeld, S. S., and E. W. Taylor. 1987. The mechanism of regulation of actomyosin subfragment 1 ATPase. *J. Biol. Chem.* 262:9984–9993.

Rüdel, R., and F. Zite-Ferenczy. 1979. Do laser diffraction studies on striated muscle indicate stepwise sarcomere shortening? *Nature (Lond.).* 278:573–575.

Schoenberg, M. 1985. Equilibrium muscle crossbridge behavior: theoretical considerations. *Biophys. J.* 48:467–475.

Schoenberg, M. 1988. The kinetics of weakly- and strongly-binding crossbridges: implications for contraction and relaxation. *In* The Molecular Mechanism of Muscle Contraction. H. Sugi and G. H. Pollack, editors. Plenum Publishing Corp., New York. 189–202.

Schoenberg, M., B. Brenner, J. M. Chalovich, L. E. Greene, and E. Eisenberg. 1984. Cross-bridge attachment in relaxed muscle. *In* Contractile Mechanisms in Muscle. G. H. Pollack and H. Sugi, editors. Plenum Publishing Corp., New York 269–284.

Schoenberg, M, and E. Eisenberg. 1985. Muscle cross-bridge kinetics in rigor and in the presence of ATP analogues. *Biophys. J.* 48:863–871.

Schoenberg, M., and J. B. Wells. 1984. Stiffness, force and sarcomere shortening during a twitch in frog semitendinosus muscle bundles. *Biophys. J.* 45:389–397.

Schoenberg, M., J. B. Wells, and R. J. Podolsky. 1974. Muscle compliance and the longitudinal transmission of mechanical impulses. *J. Gen. Physiol. (Lond.).* 64:623–642.

Siegman, M. J., T. M. Butler, S. U. Mooers, and R. E. Davies. 1976. Crossbridge attachment, resistance to stretch, and viscoelasticity in resting mammalian smooth muscle. *Science (Wash. DC).* 191:383–385.

Stein, L. A., R. P. Schwarz, P. B. Chock, and E. Eisenberg. 1979. Mechanism of actomyosin adenosine triphosphatase. Evidence that adenosine 5′ triphosphate hydrolysis can occur without dissociation of the actomyosin complex. *Biochemistry.* 18:3895–3909.

Sundell, C. L., Y. E. Goldman, and L. D. Peachey. 1986. Fine structure in near-field and far-field laser diffraction patterns from skeletal muscle fibers. *Biophys. J.* 49:521–530.

Wagner, P. D. 1984. Effect of skeletal muscle myosin light chain 2 on the Ca^{2+}-sensitive interaction of myosin and heavy meromyosin with regulated actin. *Biochemistry.* 23:5950–5956.

Wagner, P. D., and E. Giniger. 1981. Calcium-sensitive binding of heavy meromyosin to regulated actin in the presence of ATP. *J. Biol. Chem.* 256:12647–12650.

Wakabayashi, K., K. Namba, and T. Mitsui. 1984. Configurations of myosin heads in the crab striated muscle as studied by X-ray diffraction. *In* Contractile Mechanisms in Muscle. G. H. Pollack and H. Sugi, editors. Plenum Publishing Corp., New York. 237–250.

Xu, S., M. Kress, and H. Huxley. 1987. X-ray diffraction studies of the structural state of crossbridges in skinned frog sartorius muscle at low ionic strength. *J. Muscle Res. Cell Motil.* 8:39–54.

Yamamoto, T., and J. W. Herzig. 1978. Series elastic properties of skinned muscle fibres in contraction and rigor. *Pflügers Arch. Eur. J. Physiol.* 373:21–24.